Physics in Medicine & Biology

IPEM Institute of Physics and Engineering in Medicine

PAPER

# Preliminary tests of dosimetric quality and projected therapeutic outcomes of multi-phase 4D radiotherapy with proton and carbon ion beams

**Michelle Lis**[1,2,6], **Wayne Newhauser**[1,3], **Marco Donetti**[4], **Moritz Wolf**[2], **Timo Steinsberger**[2,5], **Athena Paz**[2] **and Christian Graeff**[2,*]

[1] Department of Physics and Astronomy, Louisiana State University, Baton Rouge, Louisiana, United States of America
[2] Biophysics Department, GSI Helmholtzzentrum für Schwerionenforschung GmbH, Darmstadt, Germany
[3] Department of Radiation Physics, Mary Bird Perkins Cancer Center, Baton Rouge, Louisiana, United States of America
[4] Research and Development Department, CNAO National Center for Oncological Hadrontherapy, Pavia, Italy
[5] Institute of Condensed Matter Physics, Technical University of Darmstadt, Germany
[6] Department of Electrical Engineering and Information Technology, Technical University of Darmstadt, German
[*] Author to whom any correspondence should be addressed.

**E-mail:** c.graeff@gsi.de

**Keywords:** carbon ion therapy, motion-synchronized, conformal delivery, proton therapy, projected therapeutic outcomes, multi-phase 4D dose delivery

OPEN ACCESS

RECEIVED
16 June 2021

REVISED
27 October 2021

ACCEPTED FOR PUBLICATION
5 November 2021

PUBLISHED
23 November 2021



## Abstract

*Objective*. The purpose of this study was to perform preliminary pre-clinical tests to compare the dosimetric quality of two approaches to treating moving tumors with ion beams: synchronously delivering the beam with the motion of a moving planning target volume (PTV) using the recently developed multi-phase 4D dose delivery (MP4D) approach, and asynchronously delivering the ion beam to a motion-encompassing internal tumor volume (ITV) combined with rescanning. *Approach*. We created 4D optimized treatment plans with proton and carbon ion beams for two patients who had previously received treatment for non-small cell lung cancer. For each patient, we created several treatment plans, using approaches with and without motion mitigation: MP4D, ITV with rescanning, static deliveries to a stationary PTV, and deliveries to a moving tumor without motion compensation. Two sets of plans were optimized with margins or robust uncertainty scenarios. Each treatment plan was delivered using a recently-developed motion-synchronized dose delivery system (M-DDS); dose distributions in water were compared to measurements using gamma index analysis to confirm the accuracy of the calculations. Reconstructed dose distributions on the patient CT were analyzed to assess the dosimetric quality of the deliveries (conformity, uniformity, tumor coverage, and extent of hotspots). *Main results*. Gamma index analysis pass rates confirmed the accuracy of dose calculations. Dose coverage was >95% for all static and MP4D treatments. The best conformity and the lowest lung doses were achieved with MP4D deliveries. Robust optimization led to higher lung doses compared to conventional optimization for ITV deliveries, but not for MP4D deliveries. *Significance*. We compared dosimetric quality for two approaches to treating moving tumors with ion beams. Our findings suggest that the MP4D approach, using an M-DDS, provides conformal motion mitigation, with full target coverage and lower OAR doses.

## 1. Introduction

Almost 290 000 people in the USA were diagnosed with lung or pancreatic cancer in 2019 (Siegel *et al* 2019). Of these, over 40% were diagnosed at late stages, and 5 year survivorship was only 15% for late-stage lung cancer and 8% for late-stage pancreatic cancer, respectively. Low survival rates are thought to be due, in part, to difficulty in treating these cancers (Eley *et al* 2015). Several prospective clinical trials have revealed that, for some

cancers, proton and ion beam therapies reduce the risk for treatment complications compared to photon therapies (Schulz-Ertner *et al* 2007, Malouff *et al* 2020). Carbon ion and proton therapy have been used to treat deep-seated tumors, moving tumors, and certain radioresistant tumors (Schlaff *et al* 2014, Mohamad *et al* 2017). One such radioresistant tumor, early-stage non-small cell lung cancer (NSCLC), responds well when treated with stereotactic body radiation therapy (SBRT). In contrast, late stage NSCLC treatments with photons have not demonstrated a clinical advantage with dose escalation (Chi *et al* 2010, Bradley *et al* 2015), and severe normal tissue complications have been seen in over 20% of cases (Tucker *et al* 2019). Proton and heavier ion beams have also proven advantageous relative to photon beams in cases where tumors are located near critical organs (Shipley *et al* 1995). These ion beams have emerged as effective treatments for some thoracic tumors (Liao *et al* 2018).

Considerable attention has been paid to studying the physical aspects of methods to treat moving tumors with radiation beams, particularly with photon beams (Wang *et al* 2013, Brandner *et al* 2017), but also with ion beams (Bert *et al* 2017). Approaches used in the clinic include immobilization such as breath hold (Hanley *et al* 1999) and abdominal compression (Lin *et al* 2017), free breathing with expanded safety margins such as the internal target volume (ITV) method (Shih *et al* 2004), free breathing with respiratory-synchronized beam gating (Giraud *et al* 2013), and rescanning (Bert *et al* 2009). Several well-characterized methods exist for monitoring respiration, including chest wall motion monitoring, surgically implanted radiopaque fiducial marker monitoring (Seppenwoolde *et al* 2011) and transmission photon imaging techniques (e.g. fluoroscopy). Even with these approaches, poor clinical outcomes have persisted, partly due to the dose distributions in the tumor and normal tissue being compromised by or requiring large margins due to tumor movement (Bert *et al* 2017, Meijers *et al* 2020). Motion mitigation strategies have not yet fully exploited the technical aspects of ion therapy, such as sharp gradients and fast pencil beam scanning, to deliver conformal, motion mitigated beams. To overcome these limitations, two approaches have emerged: sparing surrounding healthy tissue by minimizing tumor motion during active delivery and synchronizing beam delivery to tumor motion. To date, only a few prototypes have explored the latter approach (Saito *et al* 2009, Graeff *et al* 2013, Eley *et al* 2014, Graeff 2014). These early studies revealed promising preclinical results, but also revealed that the treatment planning and delivery processes were generally complex, machine specific, and fraught with obstacles on the path to translate them to clinical practice. Also, knowledge of the differences in dosimetric performance of these approaches was incomplete.

Further, the literature is replete with studies that explored the superior conformity and theoretical radiobiological advantages of carbon ion therapy regarding tumor control (Weber *et al* 2009, Grun *et al* 2015, Dokic *et al* 2016, Chi *et al* 2017). It has also been suggested that conformity is even more important in treatments with dose escalation (Mohamad *et al* 2017, Malouff *et al* 2020). Both radiobiological advantages and conformity are especially important for late-stage cancers, which are often radioresistant, such as pancreatic tumors and stage III/IV NSCLC (Schlaff *et al* 2014). Recent clinical outcome studies have suggested that conformal carbon ion therapy results in superior complication-free survival as compared to SBRT for stage II/III NSCLC (Shirai *et al* 2017) and for pancreatic cancers (Liermann *et al* 2020), due to the radiobiological advantages of carbon ion beams, but few clinical studies have been performed on treating late-stage lung cancers with ion therapy. A clinical outcome study at the National Institute of Radiological Sciences (NIRS) revealed that conformal carbon ion therapy resulted in nearly 55% overall survival at two years (Anzai *et al* 2020). These results are promising, but the approach appears suitable only for patients with minimal changes to the respiratory motion trajectory. A treatment planning study (Eley *et al* 2014) revealed that the beam tracking approach achieved superior dosimetric results, but introduced a high degree of technical complexity that have hindered efforts to translate the technique to clinical practice. It was not known if the dosimetric advantages of beam tracking could be obtained with a simpler approach that is more amenable to clinical translation.

The objective of this pre-clinical study was to assess the dosimetric quality of a motion-synchronized treatment delivery approach, called multi-phase 4D dose delivery (MP4D). We compared results from MP4D deliveries to those from unsynchronized approaches for treating moving tumors. We evaluated MP4D separately for proton beams and carbon ion beams using image sets from two patients who had previously received radiotherapy. Calculations were verified against measurements using two motion mitigation strategies. We assessed plan quality in terms of dose conformity, uniformity, and tumor coverage.

## 2. Materials and methods

In this study, we compared the dosimetric quality achieved by motion compensated approaches with proton and carbon ion beams. These approaches were ITV-based rescanning and MP4D (Graeff 2014, Lis *et al* 2020). For the convenience of the reader, we briefly review the previously developed methods for motion mitigation (Lis *et al* 2020) and treatment planning (Wolf *et al* 2020) that are used in this study. We also describe the experimental set-

up, as well as metrics used to characterize and compare treatment plans. We compared the relative performance of these motion mitigation methods in terms of dosimetric quantities. The results from motion mitigations approaches were compared to static deliveries without target motion (to estimate the best achievable results) and deliveries with target motion and no motion compensation (to estimate the magnitude of dose degradation caused by anatomical motion).

**2.1.4D treatment planning**

We used a research treatment planning system developed at GSI Helmholtzzentrum für Schwerionenforschung GmbH (GSI), called TRiP4D (Richter *et al* 2014). This treatment planning system extends TRiP98 (Krämer *et al* 1997, Krämer *et al* 2000) to consider patient motion during the treatment planning process. Specifically, 4DCT images were utilized to create a conformal, 4D optimized treatment plan using each motion phase. In this study, two forms of 4D-optimized treatment planning and delivery approaches were used: conformal treatment plan libraries for MP4D deliveries, and ITV-based plans for rescanned deliveries.

*2.1.1.MP4D plans*

In order to create an MP4D plan, or a library of treatment plans, one 3D sub-plan was optimized on each of the respiratory motion phases contained in the patient 4DCT image sets (introduced as '4D-rescanning' in Graeff *et al* (2014)). Each of these sub-plans were initially optimized separately to the entire prescription dose. Two forms of optimization were used for the MP4D sub-plans. First, conventional optimization was performed on a geometrical planning tumor volume (PTV) with 3 mm isotropic margins. Second, a robust optimization was performed on a clinical tumor volume with $\pm 3.5\%$ range margins (to incorporate uncertainties in Hounsfield units in the CT images) and 3 mm shifts in all cardinal directions (to consider tumor position uncertainties) (Wolf *et al* 2020), for a total of 9 scenarios in each optimization. After optimization, the number of particles in each beam spot was scaled by a weighting factor, such that the total absorbed dose of the plan library was equal to the prescribed dose (Wolf *et al* 2020). The library of optimized and weighted sub-plans was then utilized together as a single MP4D treatment plan.

*2.1.2 ITV-based plans with rescanning*

For comparison, ITV-like plans were generated on the 4DCT by optimizing a single plan simultaneously on all the motion phases of the patient 4DCT image sets (Graeff 2014, Wolf *et al* 2020). For conventional optimization, margins were considered on each 4DCT motion phase. For robust optimization, the 9 uncertainty scenarios described above were generated on each motion phase of the 4DCT image sets. This sequence incorporated motion-induced range changes into the treatment plan, also within the PTV margins or the position shift scenarios of the robust optimization. Both conventionally and robustly optimized plans were created with 10, 15 and 20 rescans to mitigate heterogeneities due to tumor motion (Bert *et al* 2009). Additionally, plans were created for deliveries to static PTVs and moving PTVs without motion compensation (interplay) by optimizing the entire treatment plan on the reference motion phase (end-exhale) of the 4DCT images.

*2.1.3 Treatment planning rationale*

We digress briefly here to explain the rationale for the treatment planning process used in this study, which is radically simplified when compared to clinical practice. This study was designed as a proof of principle, and is not representative of actual patient treatment. Two simplifications were afforded for this study to facilitate direct comparisons of various treatment strategies. Specifically, each treatment plan contained only one beam orientation, and dose constraints were not applied to OARs during the treatment planning optimization process. The primary goal of the treatment plans created for this study was to assess how tumor coverage is impacted by motion, and all treatments were designed to be substantially similar in that regard. The second goal of this study was to characterize how much normal tissue sparing could be improved with the MP4D treatment approach. The treatment plans were prepared on the basis of absorbed dose (not RBE-weighted absorbed dose) so that dose distributions could be directly compared with one another and with corresponding confirmatory measurements. An equivalent interpretation is that we used an RBE-weighted absorbed dose obtained by applying a generic, uniform RBE of unit value to all tissues for all endpoints. We purposefully avoided variation of many potentially confounding factors that might have hindered the direct comparison of dosimetric sparing of normal tissue. These include treatment factors, such as beam orientations, numbers of beams used, absorbed dose, absorbed dose rate, fractionation, and optimization of treatment plans using biological-response-corrected dose instead of absorbed dose. Host factors include tissue- and endpoint-specific RBE values, irregular intrafraction motion, and inter-fraction anatomical changes. Once the MP4D treatment approach has been shown to substantially reduce absorbed dose in healthy tissues, these other treatment and host factors will need to be evaluated.

### 2.2. Treatment delivery

The MP4D motion mitigation delivery strategy was to synchronize the delivery of the treatment plan libraries described above to the motion of a moving target. To accomplish this, we used a recently developed motion-synchronized dose delivery system (M-DDS) (Lis *et al* 2020), reviewed here for the convenience of the reader. The M-DDS extends the dose delivery system (DDS), which was originally developed and is currently used clinically at the National Center for Oncological Hadrontherapy (CNAO, Pavia Italy) and at MedAustron (Wiener Neustadt, Austria), in two major ways, namely, to provide integrated motion mitigation capabilities and to contain the necessary modularity to operate at multiple accelerator facilities. Specifically, the M-DDS is available for research studies at the radiotherapy research beamlines at CNAO and at GSI (Lis *et al* 2020). The system is embodied by a portable crate that contains eight electronics modules. Each module is a field programmable gate array (FPGA) that is dedicated to controlling one or more dose-delivery functions. These functions include transfer of beam delivery data (loading and sending of delivery information), monitoring beam intensity, monitoring beam spot position, controlling magnetic scanning of the beam, monitoring target motion and synchronizing it with beam delivery, interfacing with the accelerator timing system, initiation and termination of the irradiation, and various safety functions (Lis *et al* 2021). The motion mitigation features are implemented in two of these modules. The FPGA modules are commercial units (PCI Extensions for Instrumentation Express (PXIe), National instruments, Austin, Texas). The hardware and software interfaces to the accelerator control systems were developed in house (Lis *et al* 2020).

The MP4D approach requires continuous monitoring or prediction of the tumor motion in real time. The continuous motion signal is used to select the corresponding discrete motion phase from the library of phase-specific treatment sub-plans. The beam spots from the treatment plan corresponding to the current motion phase are delivered in their planned sequence until a change in the motion phase is detected. The next corresponding treatment plan is then selected, and beam spots are delivered starting at the location where the delivery was suspended in the previous plan. This is repeated until all beam spots in the iso-energy slice (IES) are delivered. The process continues until all IES have been delivered.

### 2.3. Patient characteristics

The treatment plans in this study were created from 10 phase 4DCTs of a patient (Patient 1) from the University of Texas MD Anderson Cancer Center in Houston, Texas and another (Patient 2) from the Champalimaud Centre for the Unknown in Lisbon, Portugal. Patient 1 was a 59 year old female, diagnosed with T2N2M1 adenocarcinoma and treated with SBRT. Patient 2 was an 83 year old male, diagnosed with stage 4 NSCLC and was treated with single fraction radiotherapy. The tumor volume for Patient 1 was 260 c.c., located in the left lower lobe of the lung at 75 mm physical depth in the reference phase. The peak-to-peak motion from the 4DCTs was estimated at 22 mm. The tumor volume for Patient 2 was 54.0 c.c., and was located in the right lower lung lobe, near the chest wall. The peak-to-peak motion was estimated to be 19.5 mm. Treatment plans for Patient 1 were delivered with both carbon ions and protons, and treatment plans for Patient 2 were delivered with protons. Patients with large tumor motion amplitudes were selected to severely test and compare motion mitigation approaches. That is, neither the selected patients nor the treatment plans were intended to be representative of typical clinical treatments.

### 2.4. Measurements and reconstructions

Before dose distribution measurements began, we performed quality assurance procedures within the available beamtime, including relative dosimetry using the methods described by Luoni *et al* (2020). Measurements included dose output constancy, and beam spot stability. Dosimetry procedures are further described by Lis *et al* (2021). The detector used in this study was calibrated according to the protocols described elsewhere (Stelljes *et al* 2015, Lis *et al* 2021).

We measured dose distributions using an ionization chamber (IC) array detector (Octavius 1500 xdr; PTW, Freiburg, Germany). The IC array detector was placed within a 5 mm thick polymethylmethacrylate (PMMA) plastic holder and PMMA slabs were placed in front (Lis *et al* 2020). Each measurement with the IC array detector was repeated three times, with the IC array detector placed at three water equivalent depths corresponding to the distal, middle, and proximal ends of the PTV or target volume: 72 mm, 96 mm, and 110 mm for Patient 1, and 95 mm, 107 mm, and 121 mm for Patient 2. The phantoms were mounted on top of a computer-controlled motorized linear stage (M-414.2PD; Physik Instrumente (PI) GmbH, Karlsruhe, Germany), which was programmed to move with a uni-axial projection of the motion from the patients' 4DCTs, thus mimicking respiratory motion.

The delivered dose distributions were reconstructed onto a water cube (to verify dose calculations against measurements) and onto the 4DCT images (to project clinical outcomes). The reconstructions were performed by parsing the delivered dose data log files from the M-DDS and motion information from motion log files (Lis

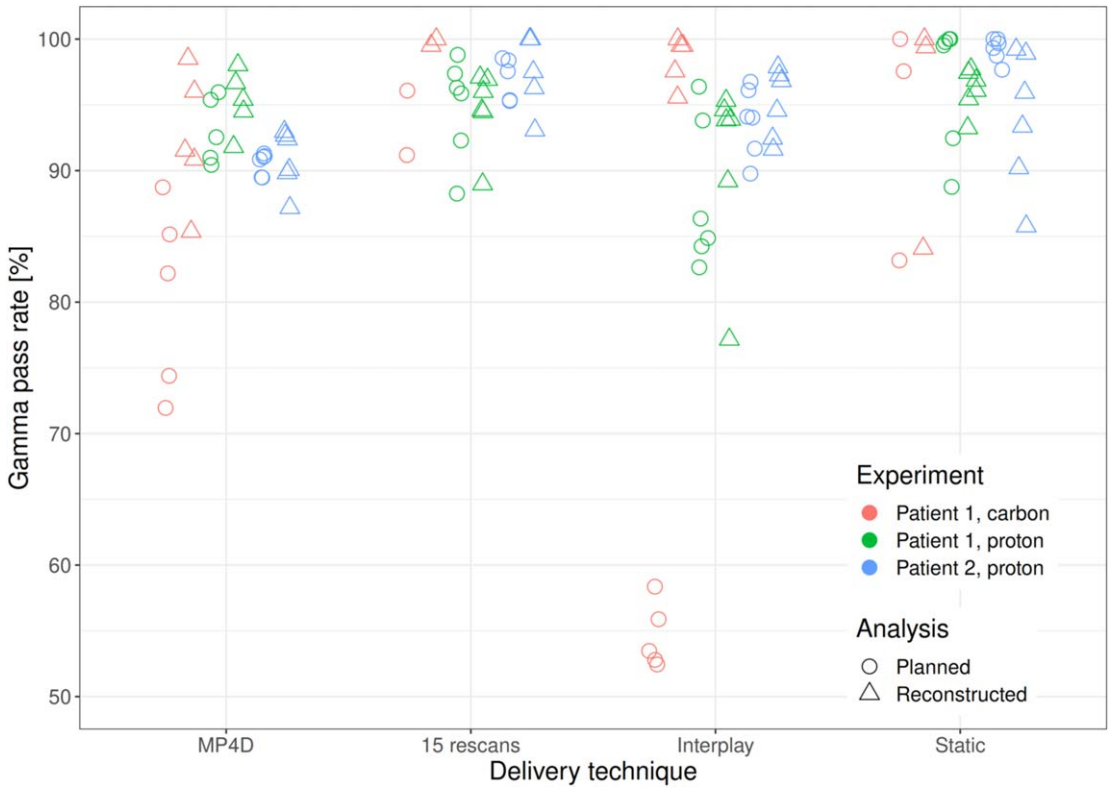


**Figure 1.** A summary of gamma index analysis results for multi-phase 4D deliveries (MP4D), ITV-based deliveries with 15 rescans, interplay and static deliveries to a water phantom with criteria of 3% dose difference and 3 mm distance to agreement. Carbon ion deliveries are represented in red for Patient 1 and proton deliveries are represented in green for Patient 1 and in blue for Patient 2. Gamma index analysis results comparing planned dose distributions to measurements are represented as circles, while results comparing reconstructed log file dose distributions measurements are represented as triangles. Dose distributions were reconstructed to a water phantom.

*et al* 2020), which provided information on the position of each delivered beam spot and of the position of the detector. The file information was then reformatted into the TRiP4D treatment plan format. TRiP4D was then used to calculate the absorbed dose distributions of the reconstructed treatment plans in water and on the 4DCT images. Dose reconstructions on the patient 4DCT images were used to assess dosimetric quality.

### 2.5. Data analysis and comparisons of dose distributions

Measured absorbed dose distributions were compared with delivery reconstructions and planned absorbed dose distributions in water using a generalized gamma index analysis. The gamma index analysis was performed to confirm the accuracy of the planned and reconstructed absorbed dose distributions, both of which were calculated. Data measured with the IC array detector was compared with planned and reconstructed distributions, calculated on a water box phantom (Stelljes *et al* 2015). Pass criteria of 3% dose difference and 3 mm local distance to agreement were applied in all cases. Gamma index pass rates of $>$90% were considered acceptable.

The ideal dosimetric characteristics of successful motion management are high uniformity, tumor coverage, and conformity, as well as the absence of hotspots. Each of these were assessed from dose volume histogram (DVH) data derived from dose distributions from treatment plans or dose reconstructions on the patient 4DCT images. The first of these, dosimetric uniformity, was assessed with the homogeneity index $HI = D5 - D95$ where $D5$ and $D95$ are the percent of the prescription doses that cover 5% and 95% of the PTV, respectively (Marks *et al* 2010). An $HI$ of 0% is ideal. Target dose coverage is the relative volume of the PTV that receives at least 95% of the prescription dose, and it is represented by $V95$. A $V95$ of 100% is ideal and 95% is commonly considered clinically sufficient target coverage of the prescription dose (Lambrecht *et al* 2018). The extent of hotspots or overdose, $V107$, is the relative target volume that receives over 107% of the prescription dose, and 0% $V107$ is ideal. Finally, dose conformity number (CN) is calculated by $CN = V_{T,p}/V_T \cdot V_{T,p}/V_p$, where $V_{T,p}$ is the volume of the target which receives a dose that is greater than or equal to the prescription dose, $V_T$ is the volume of the target, and $V_p$ is the volume in general that receives a dose that is greater than or equal to the prescription dose (Wilson *et al* 2019). It was used to assess the degree of conformity of the irradiated volume to the target volume. The ideal value on CN is 100%, but this is rarely achieved in practice.

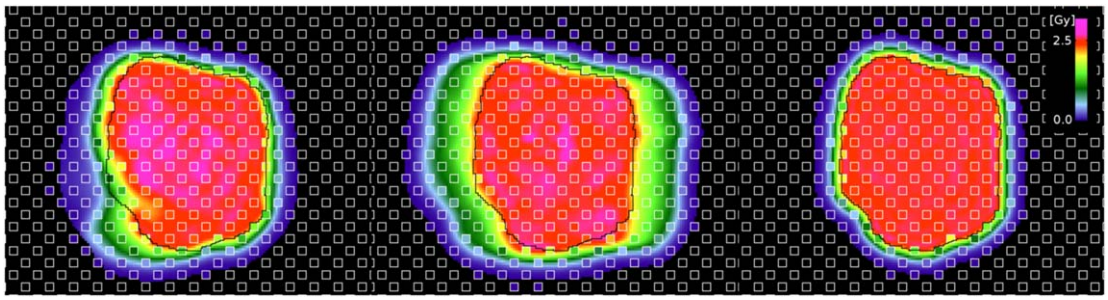


**Figure 2.** The measured dose on the matrix IC detector is superimposed on the reconstructed dose to water, each square represents a detector element, from left to right for MP4D, ITV-rescanned, and static delivery. To guide the eye, the high dose region of the static reconstruction has been added as a black contour to all cases. It should be noted that the ITV closely matches this contour, but has a larger fall-off region, while MP4D intentionally does not match this contour in water. MP4D plans are optimized on the ranges of the patient CT and will only match the CTV contour on this CT.

We omitted dose constraints on normal tissues during the plan optimization process to facilitate comparisons between delivery approaches. However, to confirm that the resulting plan libraries were still clinically realistic, DVHs for lung and heart volumes were compared to the quantitative analyses of normal tissue effects in the clinic (QUANTEC) dose criteria (Marks *et al* 2010). The selected criteria were recalculated to the used fraction size using the EQD2-formalism (Lambrecht *et al* 2018). The mean absorbed dose for symptomatic pneumonitis in the lung was $<$12 Gy for 2.5 Gy fractions, which is expected to have a 10% complication rate, and a lung $V20 <$ 30%. Only the affected lung was evaluated. For the heart, mean dose was evaluated and a $V30$ $<$ 46% was considered for pericarditis, which is expected to have a complication rate of $<$15%. The parameters were calculated for static, MP4D deliveries, and ITV-rescanned deliveries reconstructed on the patient 4D-CT, or its reference phase in the case of static delivery.

## 3. Results

All plans were optimized to a $V95$ of 100% on the nominal 4DCT, or $V95 >$ 95% in all robustness scenarios. Static plans were evaluated prior to delivery on the reference phase of the 4DCT. MP4D, ITV rescanned and interplay plans were evaluated in 4D-dose calculation on the full 4DCT. In this calculation, interplay effects were suppressed by equally distributing particles to all phases, or by fully delivering the MP4D plan to its intended phase. This dose is used as planned dose in the following.

### 3.1. Assessment of motion mitigation strategies

We assessed the dosimetric quality of MP4D deliveries with protons and carbon ions and compared the corresponding results from ITV-rescanned deliveries, static deliveries, and interplay deliveries, using the metrics described in section 2.1.

First, we used the generalized gamma index analysis (Wilson *et al* 2019) to calculate the agreement between the IC detector array measurements and planned dose distributions in water. The purpose of comparing measured and planned dose distributions was to quantify the impact motion-related dose defects. Figure 1 plots gamma index pass rates for static, interplay, ITV-based deliveries with 15 rescans, and MP4D deliveries to water. Similar analyses were performed for ITV-based deliveries with 10, 15 and 20 rescans, using carbon ions. Pass rates for deliveries for 10 and 20 rescans were below 90%, with 10 rescans showing residual interplay and 20 rescans exceeding the permissible scanning speed. ITV-based deliveries with 15 rescans were selected for further study with protons. Moreover, low pass rates were found for interplay deliveries due to the significant dose heterogeneities produced by interplay effects in the absence of motion mitigation. The pass rates for the MP4D deliveries especially for carbon were relatively lower than ITV and static deliveries, due to incomplete gating, as described further below.

Second, we quantified the agreement between reconstructed and measured dose distributions using the generalized gamma index analysis (figure 1). An example of the data used for analysis is given in figure 2. The purpose of comparing measured and reconstructed dose distributions was to validate the accuracy of the dose reconstruction method. Pass rates were generally higher for reconstructed and measured dose distributions than they were for planned and measured dose distributions. The results for static, interplay, and ITV deliveries with 15 rescans were $>$90% for 38 out of 44 experiments. For a gamma criterion of (3 mm, 4%), all reconstructed doses had a pass rate $>$90%. The average pass rates for the MP4D dose reconstructions was approximately 11% higher than the gamma index analysis results for the planned dose distributions for carbon ion dose deliveries.

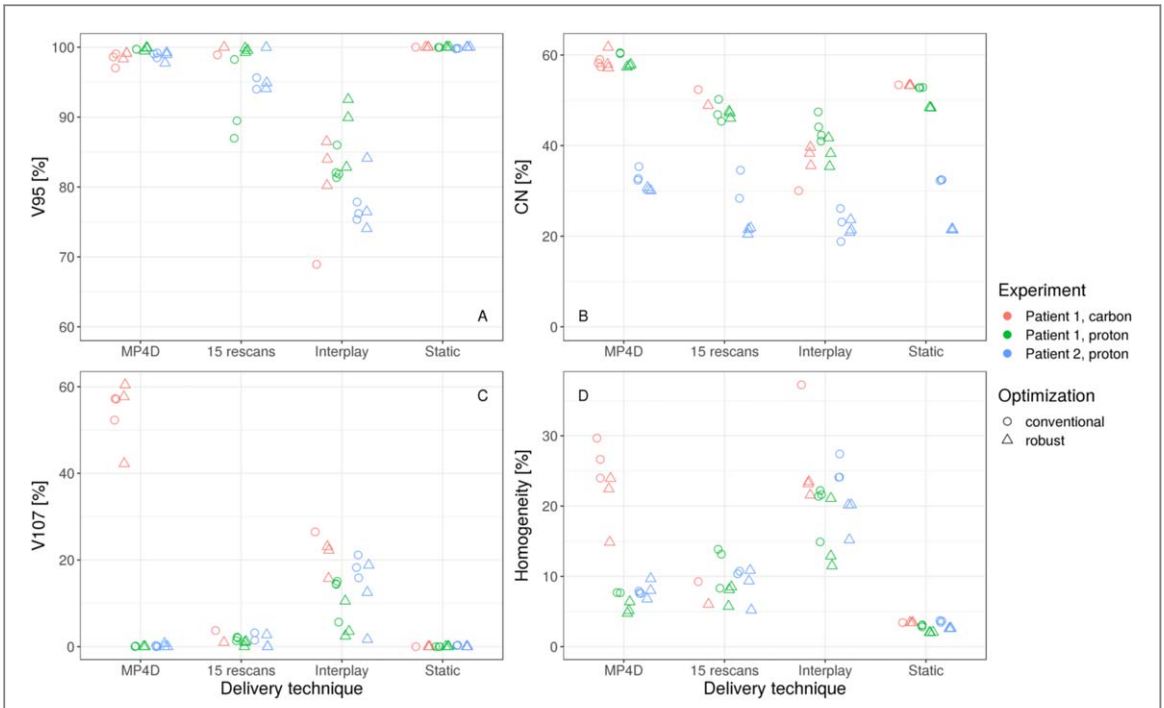


**Figure 3.** Selected delivery quality metrics, from dose-volume histogram data, including (A) dose coverage, V95, (B) conformity, CN, the (C) overdose, V107, and (D) homogeneity, HI, for carbon (Patient 1: red) and proton (Patient 1: green, Patient 2: blue) plans, for multi-phase 4D (MP4D) deliveries, ITV-based deliveries with 15 rescans, interplay, and static deliveries. Conventional 4D optimized deliveries are represented as circles and robust 4D optimized deliveries are represented as triangles. Dose reconstructions were performed on patient 4DCTs.

**Table 1.** Table of average result values for dose volume histogram (DVH) metrics for patients 1 and 2, evaluated from reconstructed dose on the patient CT. Static deliveries to a static target, multi-phase 4D deliveries (MP4D), and ITV-based rescanning deliveries were made with carbon ion and proton beams. Refer to figure 3 for an appreciation of delivery uncertainty.

| DVH metric | Patient 1 | | | | | | Patient 2 | | |
|---|---|---|---|---|---|---|---|---|---|
| Delivery strategies | Static | | MP4D | | ITV rescanned | | Static | MP4D | ITV rescanned |
| Ion | Proton | Carbon | Proton | Carbon | Proton | Carbon | Proton | | |
| Number of experiments | 6 | 3 | 5 | 5 | 6 | 2 | 6 | 6 | 5 |
| D95 (%) | 98.7 | 99.3 | 97.1 | 98.2 | 95.2 | 98.2 | 98.4 | 96.3 | 95.3 |
| V95 (%) | 100 | 100 | 99.7 | 98.5 | 95.6 | 99.4 | 99.9 | 98.8 | 95.7 |
| V107 (%) | 0 | 0 | 0 | 54.5 | 1.3 | 2.4 | 0.1 | 0.2 | 1.5 |
| CN (%) | 50.6 | 53.3 | 58.7 | 58.6 | 47.2 | 50.6 | 26.9 | 31.9 | 25.3 |
| HI (%) | 2.5 | 3.4 | 6.3 | 23.6 | 9.6 | 7.6 | 3.1 | 7.9 | 9.3 |

This suggests that the differences between planned and delivered dose distributions were mainly due to an experimental problem of incomplete beam gating through radiofrequency knockout (RFKO) rather than an inherent limitation of the conformal, MP4D approach. (The incomplete gating was a performance defect of the delivery system that was addressed subsequent to the completion of the experimental portions of this study.) This was confirmed by assessing measured particle counts during incomplete beam gating. Incomplete gating increased the delivered carbon ions by up to 9% more than were called for in the treatment plan. For protons, this effect was not fully resolved, but showed a lower impact. Gamma pass rates for MP4D were still lower than for ITV deliveries, which may be partially caused by the gating issue.

From dose reconstructions on the patient 4D-CTs, DVH data was used to calculate four dosimetric quality metrics: conformity number (CN) and homogeneity index (HI), dose coverage ($V95$) and overdose ($V107$) for each delivery. Results are summarized in table 1 and figure 3. The MP4D approach generally provided favorable outcomes, however, delivery artifacts (with incomplete beam gating) compromised carbon ion delivery results. The average CN for the MP4D deliveries was 49.2%, which are more conformal than ITV-rescanned (39.3%) and static deliveries (42.4%). Note that the conformity was in general lower for Patient 2, as the tumor volume was smaller and the relative volume of the margins increased. $V107$ results were 0.0% for static deliveries and below 2% for ITV-rescanned deliveries. In contrast, MP4D deliveries showed $V107$ values of up to 60% for

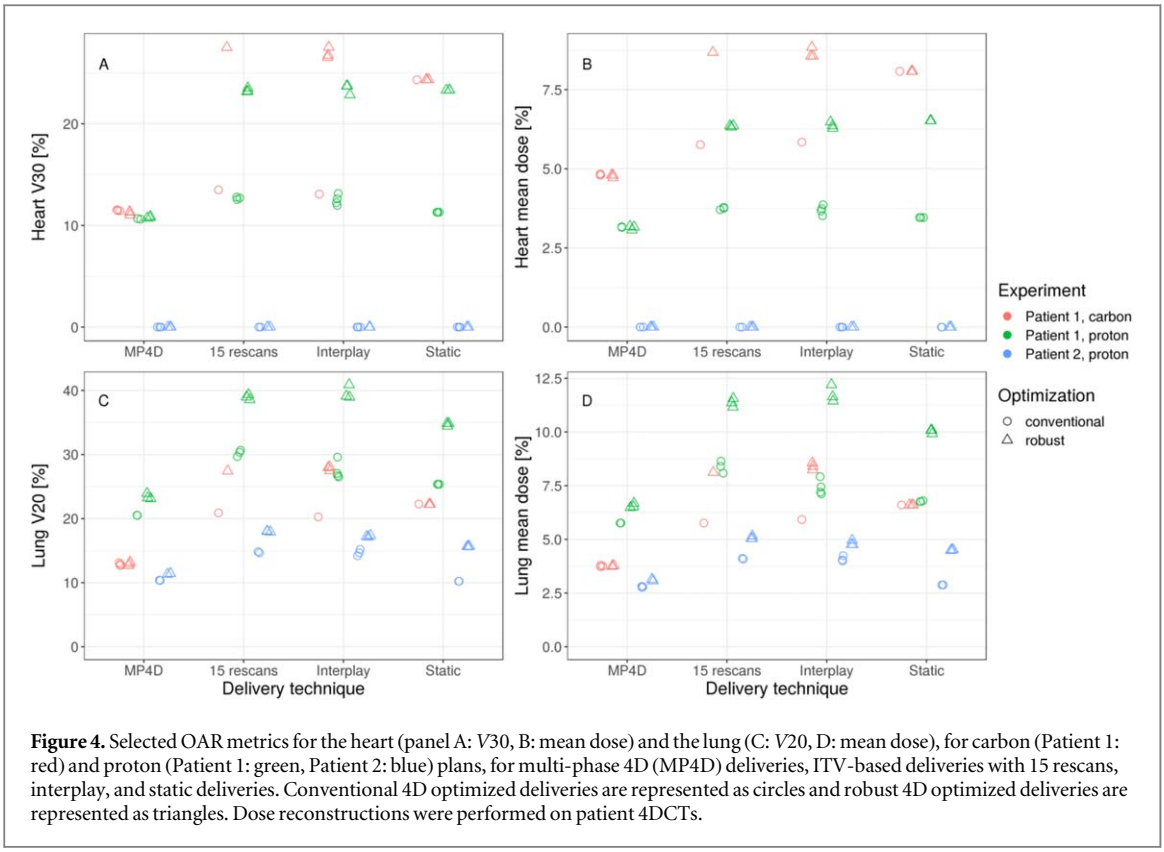


**Figure 4.** Selected OAR metrics for the heart (panel A: *V*30, B: mean dose) and the lung (C: *V*20, D: mean dose), for carbon (Patient 1: red) and proton (Patient 1: green, Patient 2: blue) plans, for multi-phase 4D (MP4D) deliveries, ITV-based deliveries with 15 rescans, interplay, and static deliveries. Conventional 4D optimized deliveries are represented as circles and robust 4D optimized deliveries are represented as triangles. Dose reconstructions were performed on patient 4DCTs.

carbon ions, likely due to incomplete beam gating. While this decreased the dosimetric quality for the MP4D deliveries, the overdose was concentrated in the target, and the conformity from carbon ion beams was still superior to the conformity of ITV-rescanned deliveries. Interplay deliveries also contained hotspots due to motion interplay effects ($V107 = 26.5\%$). Similarly, HI results for static and ITV-rescanned deliveries were, on average, below 10%, while MP4D deliveries were as high as 30% for carbon ion deliveries. In contrast, MP4D proton deliveries, which were delivered at higher speeds and required less beam gating, resulted in substantially more favorable values of *V*107 and HI. The dose coverage, *V*95, was within typical clinically acceptable ranges for all deliveries, and average (minimal) *V*95 values were 99.9% (97.0%), 100% (99.8%) and 100% (87.0%), for MP4D deliveries, static deliveries, and ITV deliveries with 15 rescans, respectively. The conventionally optimized rescanned-ITV deliveries with protons for Patient 1 showed significantly lower target coverage than other ITV irradiations, likely due to their smaller range margins compared to robust optimization. Broadly, this finding reveals that MP4D delivery resulted in the most conformal dose distributions, with a sharper dose fall off than in the ITV rescanned deliveries but with hotspots in the target.

### 3.2. DVH comparisons for delivery strategies

Log-file reconstructions for the different ions and delivery strategies were analyzed for Patient 1 by assessing DVH data. Doses to two OARs, the heart and the normal tissue of the affected lung, were compared for each of the delivery strategies, see figure 4 and table 2. Representative DVHs of Patient 1 for both ions to the target volume and to the OARs are shown in figure 5, for static deliveries, MP4D deliveries, and ITV-based deliveries with 15 rescans. In all cases, acceptable target coverage was achieved, but, for both motion mitigation strategies, lung sparing was greater for carbon ion deliveries. Lung and heart doses were highest for ITV deliveries with 15 rescans and lowest for MP4D deliveries. However, for MP4D deliveries with carbon ions, hotspots due to radiation leakage through the RFKO gating system compromised the dose delivery results to the PTV and OARs, resulting in higher doses to regions of the heart. Carbon ion deliveries also had additional dose to the heart due to the fragmentation tail. Robust optimization resulted in higher exposure of heart and lung, especially for Patient 1, due to the larger range margins of the robustness scenarios. This was not the case for robust optimization in MP4D, were range margins are possibly smeared out over the subplans in each motion phase. The robustness analysis outcome of the planned doses showed the same full target coverage of $V95 > 95\%$ in all scenarios for all plans, regardless of planning strategy, showing that the robust optimization was functioning in MP4D in spite of the more conformal dose. The exact mechanism needs to be better understood in further studies.

OAR doses were lower for MP4D deliveries compared to both static and ITV deliveries. Differences in the heart doses were smaller, but the lung showed a strong dose reduction for both patients and ions compared to

**Table 2.** OAR metrics calculated for a 2.5 Gy fraction dose to a full dose of 60 Gy for comparison to QUANTEC data. All data are given as mean (max), for the number of data points see table 1, for an appreciation of the distribution, see figure 4. Data in violation of QUANTEC criteria is printed in bold.

| DVH metric | Patient 1 | | | | | | Patient 2 | | |
|---|---|---|---|---|---|---|---|---|---|
| Delivery strategies | Static | | MP4D | | ITV rescanned | | Static | MP4D | ITV rescanned |
| Ion | Proton | Carbon | Proton | Carbon | Proton | Carbon | | Proton | |
| Lung V20 (%) | **30.0 (34.9)** | **22.2 (22.3)** | **22.6 (23.9)** | 12.9 (13.2) | **34.6 (39.3)** | **24.2 (27.4)** | 12.9 (15.7) | 10.9 (11.4) | 16.7 (18.1) |
| Lung mean dose (Gy) | 8.4 (10.1) | 6.6 (6.6) | 6.2 (6.7) | 3.8 (3.8) | 9.9 (11.6) | 6.9 (8.1) | 3.7 (4.5) | 3.0 (3.1) | 4.7 (5.2) |
| Heart V30 (%) | 17.3 (23.3) | 24.3 (24.3) | 10.7 (10.9) | 11.4 (11.5) | 18.0 (23.5) | 20.5 (27.5) | 0 | 0 | 0 |
| Heart mean dose (Gy) | 5.0 (6.5) | 8.1 (8.1) | 3.1 (3.2) | 4.8 (4.8) | 5.0 (6.4) | 7.2 (8.7) | 0 | 0 | 0 |

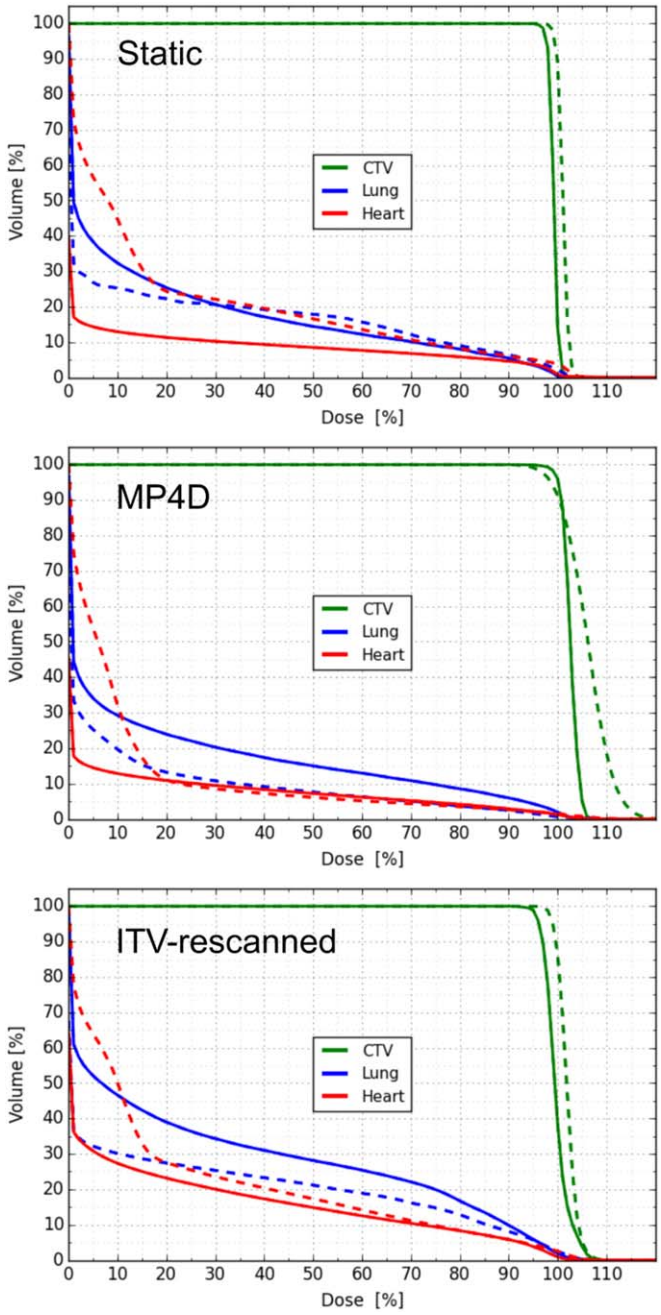


**Figure 5.** Plots of the volume doses to the target volume (green lines), the heart (red lines) and lung (blue lines) of Patient 1 for 2.5 Gy, delivered with carbon ions (represented a dashed lines) and protons (represented as solid lines) to static, 10-phase multi-phase 4D deliveries and ITV with 15 rescans (from top to bottom), reconstructed from log files on the patient 4DCTs (DDD).

the ITV delivery. Coronal and sagittal planes for each delivery are shown in figure 6, showing the reduced field size of MP4D in the main SI motion direction.

We assessed the delivery reconstructions for compliance to QUANTEC clinical dose criteria to the lung and heart for a course of 2.5 Gy fractions to a full dose of 60 Gy, see table 2. Patient 2 showed no dose to the heart and low lung exposure due to the location and smaller size of the tumor. For Patient 1, OAR doses were higher in general, and lung V20 was in violation of QUANTEC criteria for all calculations except for the carbon MP4D delivery. It should be noted that we scored only the affected lung, the opposing lung saw no dose in all cases. All other evaluated parameters for heart and lung were below the constraints, with MP4D doses showing the lowest values.

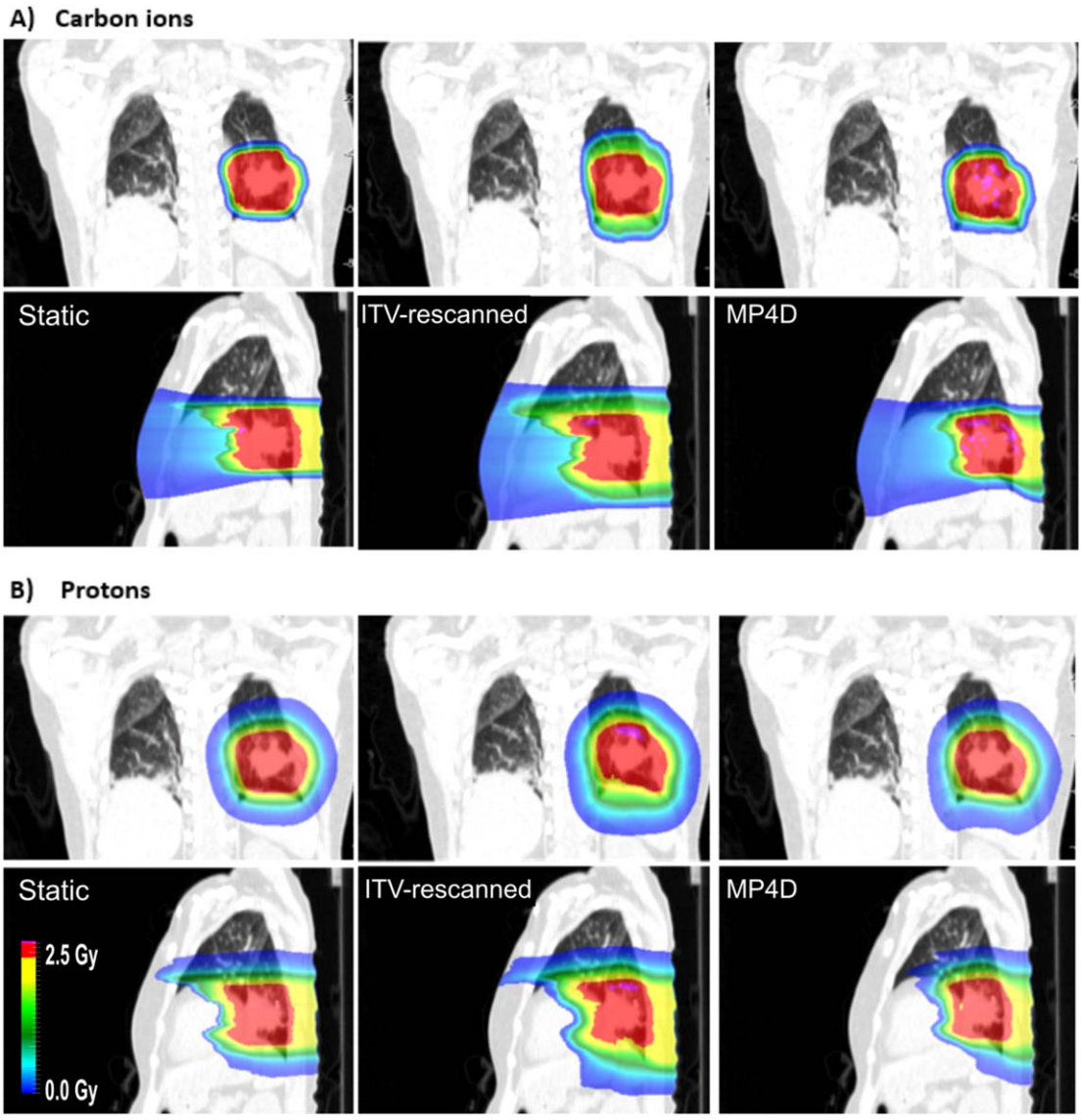


**Figure 6.** Coronal and sagittal planes of dose reconstructions on a 4DCT. Deliveries with (a) carbon ions and (b) protons are shown for static deliveries to a stationary target, ITV-based deliveries with 15 rescans, and 10-phase multi-phase 4D dose deliveries (MP4D).

## 4. Discussion

In this study, we investigated the dosimetric quality from two approaches to treating moving tumors: multi-phase 4D deliveries and ITV-based deliveries with rescanning. We retrospectively delivered patient plans to moving phantoms using both methods, with proton and carbon ions, and demonstrated the new, MP4D approach yielded superior dosimetric quality compared to other delivery approaches. The major finding of this work is that the MP4D approach can be effective at mitigating tumor motion, and potentially reducing the risk of treatment side effects. The specific results of this study suggest that the higher conformity of MP4D deliveries, combined with the sharper dose falloff of carbon ion therapy can be maintained when tumor motion is effectively mitigated, resulting in greater tissue sparing than other approaches. As expected, the lateral fall-off of carbon ions was sharper than that of protons, resulting in less lung exposure. Conversely, the carbon ion fragment tail led to a higher heart exposure for the chosen field geometry. MP4D dose reduction is strongest in the main motion direction, but also reduces range overshoot as evidenced by lower heart doses. The hotspots seen in this study for carbon ion deliveries were largely due to defects in the gating system rather than limitations of the MP4D approach.

The implication of this study is that MP4D deliveries, based on 4D optimized plan libraries, appears to be a promising approach to achieve the necessary dosimetric quality and outcomes, compared to other motion mitigation strategies with ion beams. These pre-clinical results are preliminary in nature and part of a larger effort to develop and validate a modular M-DDS.

This work is the first reported implementation of a DDS with integrated capabilities for conformal, MP4D deliveries of scanned ion beams. The results of this study are comparable to previous work in motion mitigation studies at GSI, and to delivery results for motion mitigation at the NIRS. At GSI, carbon ion planning studies have been performed to predict the dose delivery quality of motion mitigation strategies, including 4D-rescanning (here referred to as MP4D) and beam tracking (Graeff and 2014 2014). The reported results at GSI were a $V95$ of 98.5%, 72.5%, 99.4% and 98.5% for static, interplay, 4D rescanning and tracking plans, respectively. In comparison, we predicted average values of $V95$ of 100%, 98.5% and 99.4% for static deliveries, ITV-based deliveries with 15 rescans, and MP4D deliveries, respectively. As the work by Graeff *et al* (2014) was a treatment planning study, additional uncertainties, including residual motion and noisy particle delivery rates were not factored in. At NIRS, phase-controlled rescanning is used along with fluoroscopically gated deliveries. Typical dosimetric quality results listed by Mori *et al* (2014) were $D95 > 95\%$. Reported limitations included the inability to modify delivery in response to significant changes to the tumor baseline. Finally, we created and delivered both robust and conventionally optimized treatment plans for this study. For these single field deliveries, the most visible difference was a higher OAR exposure in robust optimization, which was notably absent in MP4D deliveries. A lower target coverage in conventional ITV-rescanned compared to robust plans might be indicative of the need of additional range margins.

This study has several strengths. First, the methods for assessing dosimetric quality are commonly used at ion therapy clinics, including CNAO and NIRS (Hara *et al* 2014, Mirandola *et al* 2015). This facilitates reproducing our results at other centers. Additionally, this study uses a portable and modular device (M-DDS), described in detail by Lis *et al* (2020). This will be important to address open research questions regarding more effective methods for tumor motion compensation. For this purpose, the M-DDS has several motion mitigation strategies integrated into a modular unit, including gating, ITV-based rescanning, tracking and MP4D deliveries. The M-DDS is also available at both CNAO and at GSI for research on motion mitigation. The M-DDS is a version of the DDS used clinically at CNAO and MedAustron, with modification for motion mitigation, so the clinical safety features from the original DDS are in place. Safety and performance assessments have been performed on the motion additions of the M-DDS (Lis *et al* 2020), and the plan libraries for MP4D deliveries described in this study have been delivered to phantoms at CNAO. Finally, the results of this work show that the MP4D approach is versatile enough to deliver both proton and carbon ions conformally and results in outcomes that are above the clinical standards. This presented strategy can be extended to other ion species, including helium ions and radioactive ion beams (Dokic *et al* 2016) and can be used with both synchrotrons and cyclotrons.

One limitation of this study is that it considered only two patient image sets and a limited number of treatment plans. However, this is not a serious limitation because, with the methods and infrastructure we have now demonstrated, additional studies were initiated and are underway to generate additional data that aim to inform the process of translating the M-DDS from the laboratory to the clinic. Additionally, the MP4D deliveries were performed under ideal respiration, in the absence of uncertainties due to irregular motion, such as variations in the breathing cycle patterns and an imperfect correlation between the motion signal and the actual target motion. A more exhaustive study on the benefits of conformal motion mitigation with carbon ions and protons must still be performed. Another limitation was that the RFKO extraction gating method was not fully tuned at GSI, resulting in significant hotspots in the dose distributions for the MP4D deliveries. Ideally, we would have delivered these plans at a clinical facility as well, where fast magnets dump the beam entirely during a gate. Nevertheless, the contributions of the leakage particles were quantified, and the data was analyzed with consideration of the contributions to the dose distributions. Another limitation was that the carbon ion plan libraries were optimized using absorbed dose rather than biological doses. This would have increased the complexity of the carbon ion deliveries, but also would have further increased the peak to plateau ratio for these deliveries. Previous treatment planning studies (Graeff 2017) and experiments (Gemmel *et al* 2011) have shown our capability to incorporate RBE in 4D-plans. We opted for homogeneous, directly measurable absorbed doses in this study for the sake of experimental simplicity and comparability. In future studies, we will investigate motion mitigation with RBE-weighted, physically inhomogeneous doses, as must be applied in clinical practice. This is especially true for the assessment of OAR doses, where a direct comparison to the constraints as performed here should be treated as indicative results, which will change in a complex way if RBE-weighted doses are applied. For example, the overall peak-to-plateau ratio will increase, and thus lead to more conformal delivery. In contrast, the dose tail region typically has a high RBE, which could increase OAR exposure. Further investigation on the therapeutic gain of carbon ions for NSCLC tumors are beyond the scope of this manuscript.

This study is part of a larger project to develop a modular, motion-synchronized DDS for clinical use. In the next stages, several of the limitations of this study, noted above, will be addressed. For example, MP4D deliveries will be performed with irregular motion, and the M-DDS will be expanded to correct for changes in the detected motion trajectory (so-called 'corrective tracking') and to accept diverse forms of motion trajectory information, including 3D displacement vectors. The M-DDS will later be transferred to CNAO for pre-clinical testing.

## 5. Conclusions

The results of this work support that the multi-phase 4D dose delivery (MP4D) approach can deliver ion beam treatments with favorable treatment quality compared to other motion mitigation approaches. The M-DDS used in this work is modular, portable design that has a variety of motion mitigation strategies incorporated. Compared to ITV-based deliveries with rescanning, the MP4D approach is more conformal, potentially resulting in more favorable treatment outcomes.

## Acknowledgments

We would like to thank U Weber and C Schuy for providing our group with the detectors and phantoms used in this study. We would also like to thank T Friedrich for his feedback on calculating therapeutic outcomes. The research presented here is a result of a R&D project experiment SBIO at the beam line SIS-18 in the frame of FAIR Phase-0 supported by the GSI Helmholtzzentrum für Schwerionenforschung in Darmstadt (Germany).

## Conflict of interest

The authors declare that the research was conducted in the absence of any commercial or financial relationships that could be construed as a potential conflict of interest.

## Author contributions

CG, MD, WN devised the project. ML CG and WN wrote the manuscript. ML and MD developed the M-DDS that is the device validated in this work. WN and CG provided scientific direction and supervised this work. ML, MW, TS, AP and CG performed experiments and gathered data. ML, MW, CG and TS contributed to analyzing the data of this study, including log file reconstructions and data post-processing procedures. All authors participated in the preparation of the manuscript.

## Funding

This project has received funding from the European Union's Horizon 2020 research and innovation programme under the Marie Skłodowska-Curie grant agreement No 675265, OMA—Optimization of Medical Accelerators, from the Charles E. Coates travel award (LSU), and from the August Family Professorship (LSU).

## ORCID iDs

Michelle Lis https://orcid.org/0000-0001-9117-0985
Moritz Wolf https://orcid.org/0000-0001-9250-2478
Christian Graeff https://orcid.org/0000-0002-5296-7649

## References

Anzai M *et al* 2020 Safety and efficacy of carbon-ion radiotherapy alone for stage III non-small cell lung cancer *Anticancer Res.* **40** 379–86
Bert C and Herfarth K 2017 Management of organ motion in scanned ion beam therapy *Radiat. Oncol.* **12** 170
Bert C *et al* 2009 *Rescanning to Mitigate the Impact of Motion Inscanned Particle Therapy,in GSI Scientific Report 2008* ed K Große (Darmstadt, Germany: GSI) p 397
Bradley J D *et al* 2015 Standard-dose versus high-dose conformal radiotherapy with concurrent and consolidation carboplatin plus paclitaxel with or without cetuximab for patients with stage IIIA or IIIB non-small-cell lung cancer (RTOG 0617): a randomised, two-by-two factorial phase 3 study *Lancet Oncol.* **16** 187–99
Brandner E D *et al* 2017 Motion management strategies and technical issues associated with stereotactic body radiotherapy of thoracic and upper abdominal tumors: a review from NRG oncology *Med. Phys.* **44** 2595–612
Chi A *et al* 2010 Systemic review of the patterns of failure following stereotactic body radiation therapy in early-stage non-small-cell lung cancer: clinical implications *Radiother. Oncol.* **94** 1–11
Chi A *et al* 2017 Comparison of photon volumetric modulated arc therapy, intensity-modulated proton therapy, and intensity-modulated carbon ion therapy for delivery of hypo-fractionated thoracic radiotherapy *Radiat. Oncol.* **12** 132
Dokic I *et al* 2016 Next generation multi-scale biophysical characterization of high precision cancer particle radiotherapy using clinical proton, helium-, carbon- and oxygen ion beams *Oncotarget* **7** 56676–89
Eley J G *et al* 2014 4D optimization of scanned ion beam tracking therapy for moving tumors *Phys. Med. Biol.* **59** 3431–52
Eley J G *et al* 2015 Robustness of target dose coverage to motion uncertainties for scanned carbon ion beam tracking therapy of moving tumors *Phys. Med. Biol.* **60** 1717–40

Gemmel A *et al* 2011 Calculation and experimental verification of the RBE-weighted dose for scanned ion beams in the presence of target motion *Phys. Med. Biol.* **56** 7337–51
Giraud P and Houle A 2013 Respiratory gating for radiotherapy: main technical aspects and clinical benefits *ISRN Pulmol.* **2013** 519602
Graeff C *et al* 2013 A 4D-optimization concept for scanned ion beam therapy *Radiother. Oncol.* **109** 419–24
Graeff C 2014 Motion mitigation in scanned ion beam therapy through 4D-optimization *Phys. Med* **30** 570–7
Graeff C 2017 Robustness of 4D-optimized scanned carbon ion beam therapy against interfractional changes in lung cancer *Radiother. Oncol.* **122** 387–92
Grun R *et al* 2015 Assessment of potential advantages of relevant ions for particle therapy: a model based study *Med. Phys.* **42** 1037–47
Hanley J *et al* 1999 Deep inspiration breath-hold technique for lung tumors: the potential value of target immobilization and reduced lung density in dose escalation *Int. J. Radiat. Oncol.*Biol.*Phys.* **45** 603–11
Hara Y *et al* 2014 Application of radiochromic film for quality assurance in the heavy-ion beam scanning irradiation system at HIMAC *Nucl. Instrum. Methods Phys. Res.* B **331** 253–6
Krämer M *et al* 2000 Treatment planning for heavy-ion radiotherapy: physical beam model and dose optimization *Phys. Med. Biol.* **45** 3299–317
Krämer M and Jäkel O 1997 Therapy Planning for Heavy Ion Irradiation
Lambrecht M *et al* 2018 Radiation dose constraints for organs at risk in neuro-oncology; the European particle therapy network consensus *Radiother. Oncol.* **128** 26–36
Liao Z *et al* 2018 Bayesian adaptive randomization trial of passive scattering proton therapy and intensity-modulated photon radiotherapy for locally advanced non–small-cell lung cancer *J. Clin. Oncol.* **36** 1813–22
Liermann J *et al* 2020 Carbon ion radiotherapy as definitive treatment in non-metastasized pancreatic cancer: study protocol of the prospective phase II PACK-study *BMC Cancer* **20** 947
Lin L *et al* 2017 Evaluation of motion mitigation using abdominal compression in the clinical implementation of pencil beam scanning proton therapy of liver tumors *Med. Phys.* **44** 703–12
Lis M *et al* 2021 A facility for the research, development, and translation of advanced technologies for ion-beam therapies *J. Instrum.* **16** T03004
Lis M *et al* 2020 A modular dose delivery system for treating moving targets with scanned ion beams: Performance and safety characteristics, and preliminary tests *Phys Med* **76** 307–16
Lis M *et al* 2021 Dosimetric validation of a modular system to treat moving tumors using scanned ion beams that are synchronized with anatomical motion *Front. Oncol.* **11** 712126
Lis M *et al* 2021 A modular system for treating moving anatomical targets with scanned ion beams at multiple facilities; pre-clinical testing for quality and safety of beam delivery *Front. Oncol.* **11** 620388
Luoni F *et al* 2020 Beam monitor calibration for radiobiological experiments with scanned high energy heavy ion beams at FAIR *Front. Phys.* **8** 397
Malouff T D *et al* 2020 Carbon ion therapy: a modern review of an emerging technology *Front. Oncol.* **10** 82
Marks L B *et al* 2010 Use of normal tissue complication probability models in the clinic *Int. J. Radiat. Oncol.*Biol.*Phys.* **76** S10–9
Meijers A *et al* 2020 Evaluation of interplay and organ motion effects by means of 4D dose reconstruction and accumulation *Radiother. Oncol.* **150** 68–274
Mirandola A *et al* 2015 Dosimetric commissioning and quality assurance of scanned ion beams at the Italian National Center for Oncological Hadrontherapy *Med. Phys.* **42** 5287–300
Mohamad O *et al* 2017 Carbon ion radiotherapy: a review of clinical experiences and preclinical research, with an emphasis on DNA damage/repair *Cancers* **9** 66
Mori S *et al* 2014 A serial 4DCT study to quantify range variations in charged particle radiotherapy of thoracic cancers *J. Radiat. Res.* **55** 309–19
Richter D *et al* 2014 Four-dimensional patient dose reconstruction for scanned ion beam therapy of moving liver tumors *Int. J. Radiat. Oncol. Biol. Phys.* **89** 175–81
Saito N *et al* 2009 Speed and accuracy of a beam tracking system for treatment of moving targets with scanned ion beams *Phys. Med. Biol.* **54** 4849–62
Schlaff C D *et al* 2014 Bringing the heavy: carbon ion therapy in the radiobiological and clinical context *Radiat. Oncol.* **9** 88
Schulz-Ertner D and Tsujii H 2007 Particle radiation therapy using proton and heavier ion beams *J. Clin. Oncol.* **25** 953–64
Seppenwoolde Y *et al* 2011 Treatment precision of image-guided liver SBRT using implanted fiducial markers depends on marker–tumour distance *Phys. Med. Biol.* **56** 5445–68
Shih H A *et al* 2004 Internal target volume determined with expansion margins beyond composite gross tumor volume in three-dimensional conformal radiotherapy for lung cancer *Int. J. Radiat. Oncol.*Biol.*Phys.* **60** 613–22
Shipley W U *et al* 1995 Advanced prostate cancer: the results of a randomized comparative trial of high dose irradiation boosting with conformal protons compared with conventional dose irradiation using photons alone *Int. J. Radiat. Oncol.*Biol.*Phys.* **32** 3–12
Shirai K *et al* 2017 Clinical outcomes using carbon-ion radiotherapy and dose-volume histogram comparison between carbon-ion radiotherapy and photon therapy for T2b-4N0M0 non-small cell lung cancer—a pilot study *PLoS One* **12** e0175589
Siegel R L, Miller K D and Jemal A 2019 Cancer statistics *CA: A Cancer J. Clin.* **69** 7–34
Stelljes T S *et al* 2015 Dosimetric characteristics of the novel 2D ionization chamber array OCTAVIUS detector 1500 *Med. Phys.* **42** 1528–37
Tucker S L *et al* 2019 Validation of effective dose as a better predictor of radiation pneumonitis risk than mean lung dose: secondary analysis of a randomized trial *Int. J. Radiat. Oncol.*Biol.*Phys.* **103** 403–10
Wang Y *et al* 2013 Assessment of respiration-induced motion and its impact on treatment outcome for lung cancer *BioMed Res. Int.* **2013** 872739
Weber U and Kraft G 2009 Comparison of carbon ions versus protons *Cancer J.* **15** 325–32
Wilson L J, Newhauser W D and Schneider C W 2019 An objective method to evaluate radiation dose distributions varying by three orders of magnitude *Med. Phys.* **46** 1888–95
Wolf M *et al* 2020 Robust treatment planning with 4D intensity modulated carbon ion therapy for multiple targets in stage IV non-small cell lung cancer *Phys. Med. Biol.* **65** 215012